Oxidation of Cholesterol Does Not Alter Significantly its Uptake into High Density Lipoprotein Particles

Topi Karilainen,[1] Štěpán Timr,[2] Ilpo Vattulainen,[1,3] and Pavel Jungwirth[2,1*]*

[1]Department of Physics, Tampere University of Technology, P. O. Box 692, FI-33101 Tampere, Finland

[2]Institute of Organic Chemistry and Biochemistry, Academy of Sciences of the Czech Republic, Flemingovo nám. 2, 16610 Prague 6, Czech Republic

[3]MEMPHYS-Center for Biomembrane Physics, University of Southern Denmark, Odense, Denmark

[*]*Corresponding authors: ilpo.vattulainen@tut.fi (I.V.) and pavel.jungwirth@uochb.cas.cz (P.J.)*

Keywords: oxysterol, molecular dynamics, umbrella sampling, replica exchange

Abstract

Using replica exchange umbrella sampling we calculated free energy profiles for uptake of cholesterol and one of its oxysterols (7-ketocholesterol) from an aqueous solution into a high density lipoprotein particle. These atomistic molecular dynamics simulations show that both sterols are readily taken up from the aqueous solution with comparable free energy minima at the surface of the particle of -17 kcal/mol for cholesterol and -14 kcal/mol for 7-ketocholesterol. Moreover, given its preferred position at the particle surface, 7-ketocholesterol is expected to be able to participate directly in biological signaling processes.

Introduction

High density lipoprotein (HDL) takes up excess cholesterol from cells, carries it into the blood circulation as cholesteryl ester, and unloads it in the liver, where it is metabolized.[1] This process of reverse cholesterol transport helps prevent cardiovascular disease by removing cholesterol from foam cells, thus working against the formation of atherosclerotic plaques. High serum HDL levels are associated with reduced risk of cardiovascular disease, and increasing HDL in circulation is recognized as a potential therapeutic target.[2]

Mature HDL particles are spherical and have radii of approximately 5 nm.[3] They consist of a surface phospholipid layer in which typically three to five amphiphilic apolipoproteins are embedded, and a hydrophobic core of triglycerides and esterified cholesterol.[4] Some free cholesterol is also present in the surface layer.

Oxidation of HDL impairs its ability to take up cholesterol from cells, which can prevent it from performing its atheroprotective function.[5] HDL is known to carry lipid oxidation products *in vivo*.[6] The foam cells that make up the atherosclerotic plaque contain reactive oxygen species (ROS), and the lipids and proteins that constitute HDL are prone to oxidation by ROS.[7] A wide range of oxidized lipids and oxidized amino acid residues of apolipoproteins have been identified in atherosclerotic lesions,[8] and they are implicated in loss of HDL function.[9,10]

Oxysterols are oxidized derivatives of cholesterol, which are believed to have a signaling role in cholesterol transport.[11] Oxysterols can be produced from cholesterol enzymatically, by the influence of ROS, or via autoxidation. There exists a diverse array of oxysterols with hydroxyl or carboxyl groups at different positions in the molecule. 7-ketocholesterol is one of the more abundant oxysterols, which is also used as a measure of radical cholesterol oxidation.[8] The formulas of cholesterol and 7-ketocholesterol are shown in Figure 1. Once taken up by HDL, the

exact location of 7-ketocholesterol in the lipoprotein particles has implications for its ability to participate in signaling while being transported in the bloodstream by HDL. There is experimental evidence for uptake of 7-ketocholesterol into HDL,[12] but direct observations of neither its radial partitioning in lipoprotein particles nor its positioning along the phospholipid layer and with respect to apolipoproteins are available. Atomistic molecular dynamics (MD) simulations can provide a detailed insight into this behavior.

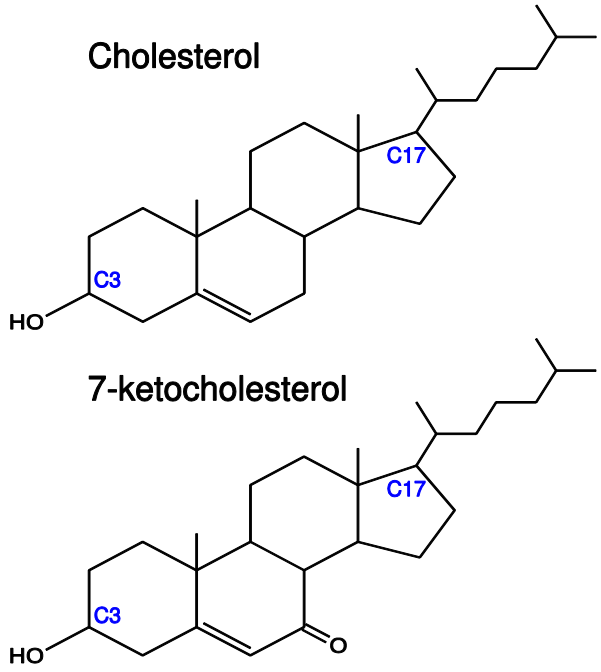

Figure 1. *Structures of cholesterol and 7-ketocholesterol. The carbon atoms labeled C3 and C17 are used to define the director of the molecule (see methods for details).*

Previously, atomistic and coarse-grained MD simulations have been used successfully to elucidate the structures and numerous properties of HDL and low density lipoprotein (LDL) particles.[13–17] They have also turned out to be very useful in unlocking how HDL and LDL levels can be modulated through the action of drugs such as anacetrapib.[18] Altogether previous studies highlight that molecular-scale simulations can provide considerable added value to experimental

work to clarify phenomena associated with nanoscale systems, lipoproteins being an excellent example of this type.

In this work, we applied replica exchange umbrella sampling (REUS)[19] to extract the free energy profiles of cholesterol or 7-ketocholesterol along their distance *r* from the center of HDL with the aim to characterize the difference between the uptake of normal vs. oxidized cholesterol to HDL. In the following, we outline the methodology and present the results from REUS applied to uptake of cholesterol or 7-ketocholesterol into an HDL particle, showing that both sterols are readily adsorbed by this particle in a similar way.

Computational methods

We prepared the atomistic model of a mature spherical HDL particle, based on the lipid and apolipoprotein A-I (apoA-I) composition and apoA-I structural arrangement determined previously.[4] Our model consists of 133 1-palmitoyl-2-oleoylphosphatidylcholine (POPC) molecules as the surface phospholipid monolayer and 106 cholesteryl oleate (CO) molecules as the hydrophobic core lipids. Four apoA-I chains were placed on the surface in a twisted cage-like arrangement with antiparallel alpha helices, as determined previously.[4] The radius of HDL, defined as the radial distance to the interface where the number densities of atoms of HDL and water are equal, is 4.6 nm in our model. The number densities of the components of HDL are shown in Figure 2, demonstrating the distribution of individual species in the particle. The lipid headgroup and apolipoprotein region extends up to a distance of 6 nm from the center of the HDL particle.

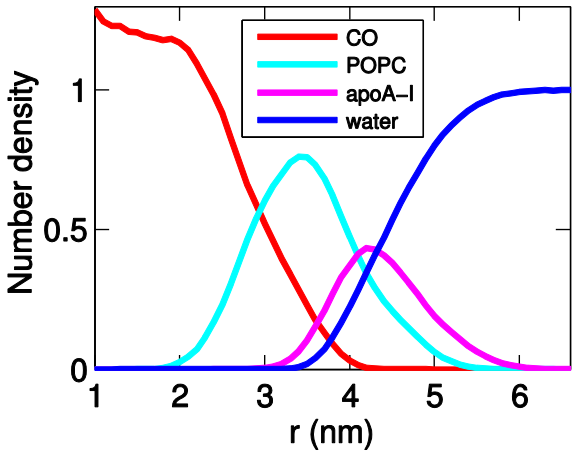

Figure 2. *The number densities of the individual components of the HDL particle and of water. The y axis is normalized so that the number density of bulk water equals one.*

We refer to cholesterol and 7-ketocholesterol as the solutes in umbrella sampling simulations. For both solutes, we made two independent REUS simulations with 37 umbrella windows, spaced 0.15 nm apart along the reaction coordinate r, which we define as the distance between the centers of mass of HDL and the solute. The simulation time was 60 ns per window. For both solutes, one independent simulation had the solute headgroup initially pointing "up" (toward the water phase, away from the HDL center), while the other had it initially pointing "down". With standard umbrella sampling (no replica exchange), we made the same preparations as with REUS and simulated 20 ns per window. Finally, we made two additional REUS simulations of 220 ns and 150 ns per window in the region of 2.5 nm $< r <$ 3.8 nm for cholesterol, where the initial orientations alternated between "up" and "down" in adjacent windows. A snapshot of the 7-ketocholesterol at the HDL surface, r = 3.4 nm, is shown in Figure 3.

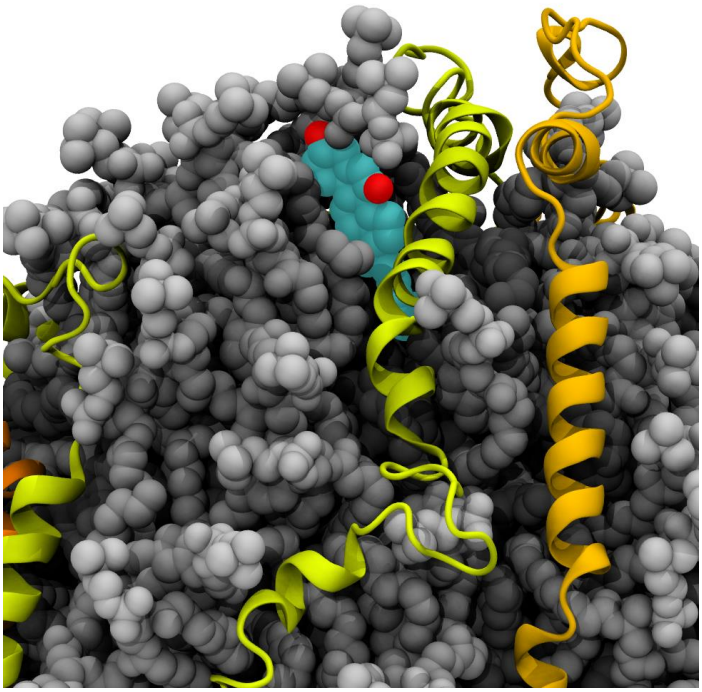

Figure 3. *A snapshot of 7-ketocholesterol (carbon atoms cyan, oxygen atoms red, and hydrogen atoms not shown) at the surface of HDL, where r = 3.4 nm (surface view at a part of the particle). The apoA-I proteins are shown in yellow and orange. POPC headgroups, POPC hydrocarbon tails, and CO molecules are shown in shades of gray in this order from lightest to darkest. The tails of two POPC molecules and all water molecules are omitted from the image in order to better show the 7-ketocholesterol molecule. In this position, both oxygen atoms of 7-ketocholesterol are in the headgroup region.*

We used the OPLS-AA force field for lipids, ions, and proteins[20] together with the TIP3P water model.[21] The simulation temperature was maintained at 310 K with the Nosé-Hoover thermostat[22,23] and the pressure at 1 bar with the Parrinello-Rahman barostat.[24] The time constant for temperature coupling was set to 0.4 ps. For pressure coupling, the time constant was 4 ps and the compressibility was 4.5×10^{-5} bar^{-1}. We used periodic boundary conditions in all directions. Bond lengths were constrained by the linear constraint solver (LINCS) algorithm.[25] The Lennard-

Jones interaction cutoff was 1.0 nm, and electrostatic interactions were calculated by the particle mesh Ewald method[26] with a grid spacing of 0.12 nm and Coulomb cut-off of 1.0 nm. The simulation time step was 2 fs.

Umbrella sampling is a widely used technique in molecular dynamics simulations to study the free energy along a given pathway.[27,28] A series of simulations with biasing potentials at different points along the pathway provide the free energy profile once the effect of the biasing potential is separated out by a suitable method such as the weighted histogram analysis.[29] Although conventional umbrella sampling has been successfully used in many applications, it may suffer from poor convergence if high free energy barriers are present in degrees of freedom perpendicular to the reaction coordinate.[30,31] These barriers cause long relaxation times, which may result in substantial sampling errors. The convergence of free energy profiles can be accelerated by combining umbrella sampling with Hamiltonian replica exchange in umbrella potentials. This REUS technique[19] (also known as window exchange[32] or bias exchange[33] umbrella sampling or, alternatively, distance replica exchange[34]) achieves enhanced sampling of orthogonal degrees of freedom by allowing replicas starting from different initial geometries to migrate along the reaction coordinate.

REUS has been used with success to study oligopeptide conformations[19] and self-assembly,[35] DNA base stacking,[36] kink-turns in double-stranded RNA,[37] transmembrane helix assembly,[32] prediction of protein-ligand binding structures,[38,39] or a conformational transition of a membrane transporter.[33] Extended to two dimensions, the technique has been also applied to studies of ion and substrate binding to proteins,[40,41] recovery from inactivation of ion channels,[42] and transmembrane helix assembly.[43] A method very similar to REUS has also been utilized for

obtaining the free energy profile of a small solute across a lipid bilayer, leading to an enhancement of the rate of convergence by up to a factor of four in comparison to standard umbrella sampling.[44]

A customized version of the GROMACS 4.6.5 molecular dynamics code[45] was used in the present study to perform REUS simulations. The force constant for the umbrella potentials was 1000 kJ mol^{-1} and the interval between replica exchange attempts was 2 ps. We made the free energy profiles with the weighted histogram analysis method[29] for two different sets of starting geometries of the sterol molecule (as mentioned above). We then calculated the error bars for the combination of these two runs with the bootstrap analysis method and placed them on top of the average of the two free energy profiles (see Figure 4).[46] To assess the convergence of the free energies, we calculated the free energy change ΔG from r = 3.4 nm (the point of minimum free energy) to r = 6.8 nm (the water phase) at different lengths of each simulation to obtain the plot of ΔG versus time.

To quantify the sampling of solute orientations, we defined the solute director as the vector from cholesterol carbon atoms C17 to C3, where C17 is located in the five-carbon ring and is connected to the lipid tail and C3 is the carbon atom connected to the hydroxyl group. We then define the effective normal of HDL as the vector from the COM of HDL to the midpoint of the director and the orientational angle θ as the angle between the director and the effective normal. We then divided r into 0.1 nm bins and calculated the angle distribution over the length of the simulation in each bin.

To identify free energy barriers orthogonal to r during REUS, we calculated the transmission factor ratio along r, T_r^{ratio}, as shown by Neale et al.[44] The transmission factor T_r shows how well replicas are able to move along r by comparing how often they travel across a region of defined width, Δr, and how often a replica enters the region. The quantity T_r^{ratio} compares T_r obtained

from REUS to T_r^{random}, the transmission factor calculated from random walks with the acceptance probabilities taken from REUS. We used a value of Δr = 0.9 nm in our calculations.

Results and discussion

The free energy profiles obtained from the potential of mean force calculations with REUS are shown in Figure 4. The most important feature of the profile is the free energy decrease of moving the solute from the water phase (at r = 6.8 nm) to the phospholipid layer of HDL (at r = 3.4 nm). This energy is −17 kcal mol^{-1} for cholesterol and −14 kcal mol^{-1} for 7-ketocholesterol. Both cholesterol and 7-ketocholesterol show a steeply increasing free energy curve between 3.4 nm and 5 nm, which indicates that both solutes are readily adsorbed into the HDL surface layer once contact is made. This is in agreement with the experimental observation that 7-ketocholesterol is taken up by HDL and accumulates in cells if cholesterol efflux is prevented.[12]

The free energies from independent simulations with opposite starting orientations are in good agreement with each other at 3.4 nm < r < 6.8 nm for both solutes. Then, at 3.4 nm, the two profiles for cholesterol simulations start deviating as the simulation with cholesterol initially in "headgroup down" orientation has a free energy decrease of approximately 3 kcal mol^{-1} going from r = 3.4 nm to r = 2.8 nm. This is surprising because it means that there is a favorable free energy decrease although the cholesterol headgroup is losing contact with the POPC headgroup region. One would expect that when the cholesterol molecule has its headgroup turned towards the HDL core, both the hydroxyl headgroup and the lipid tail of cholesterol are in an unfavorable environment. However, analysis of the REUS simulation at r = 2.8 nm reveals that when cholesterol is initially placed headgroup down, the hydrogen atom in the cholesterol headgroup finds a hydrogen bond acceptor from the cholesteryl esters, while the side chains of hydrophobic amino acids provide a nonpolar setting for the cholesterol tail at the lower edge of the POPC headgroup region. In this

way, both ends of cholesterol find a fitting local environment. The surface coverage of apoA-I in HDL is 50 %. No more than 89 out of its 243 residues are hydrophobic, therefore, suitable places for cholesterol to orient in this way are available in only 20 % of the HDL surface. According to our free energy results for the "headgroup down" simulation, it is possible that cholesterol molecules are stable in a nonstandard orientation in such areas, which gives rise to the local orientational variations at the POPC/apoA-I surface.

The discussion above concerns the results from 60 ns simulations shown in the main plot in Figure 4. To improve convergence in the region around r = 3.4 nm for cholesterol we made two additional REUS simulations of 150 ns and 220 ns per window in the range 2.5 nm < r < 3.8 nm. The result is shown in the inset of Figure 4, where the additional simulations are denoted "CHOL refined 1" and "CHOL refined 2". The cholesterol curves from the main plot are repeated in the inset.

The main result of these significantly longer additional simulations is the observation that the convergence of the free energy in this region becomes reasonable at r > 2.8 nm, but falls short of being acceptable at smaller r. According to the extended simulations, the minimum of free energy is still found at r = 3.4 nm, but the energy cost of cholesterol penetrating at least 0.5 nm deeper into the HDL particle is small. Therefore, one could expect to find cholesterol molecules at distances from 2.9 nm to 3.4 nm from the center of HDL. On the basis of this result from the refined simulations, as well as the above discussion of the local environment of the cholesterol molecule, and studies where the position of cholesterol was determined to be in the headgroup region of HDL and HDL-like lipid droplets,[13] we conclude that the low free energy pertinent to the cholesterol "headgroup down" simulation at r < 3.4 is a local effect arising from limited sampling and is not representative of the global free energy.

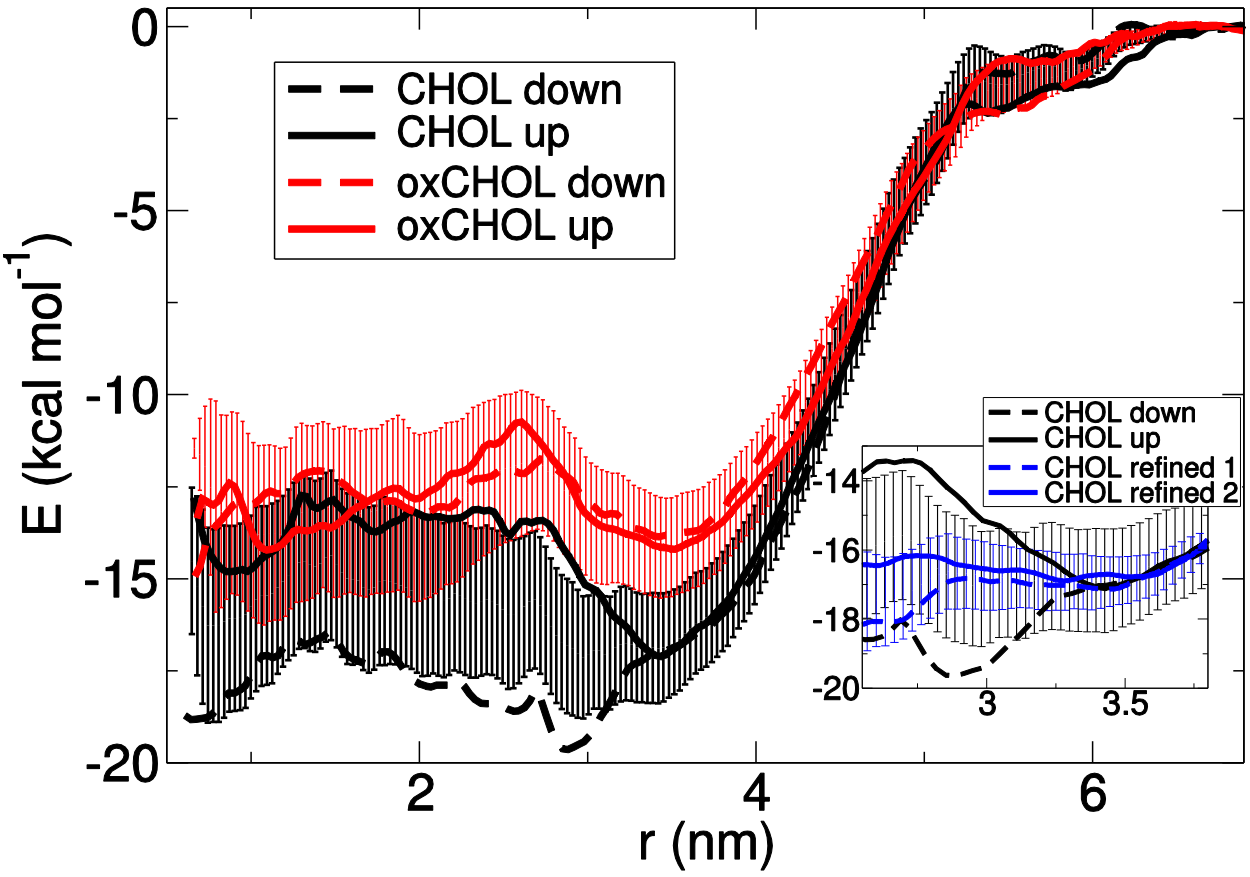

Figure 4. *Free energy as a function of distance from the center of HDL after 60 ns of REUS in two independent simulations of cholesterol (CHOL) and 7-ketocholesterol (oxCHOL) and refinement by additional simulations for cholesterol at 2.5 nm < r < 3.8 nm (inset). The initial orientation of the solute is marked as (headgroup) down or (headgroup) up in the legend. The free energy at r = 6.8 nm was set to zero. As the solute moves toward HDL, at 5 nm < r < 6.5 nm, contacts of solute with the diffuse surface of HDL cause small differences in the PMF. In the region from 3.4 nm to 5 nm, the profiles of each solute are converged. In the hydrophobic core of the HDL particle at r < 3.4 nm, the free energy has a large uncertainty because of long autocorrelation times. We consider r = 3.4 nm to be the distance of minimum energy, although in the case of unoxidized cholesterol, the energies from two independent simulations diverge at smaller r (see discussion).*

The free energy difference between cholesterol and 7-ketocholesterol at r = 3.4 nm from the HDL center of 3 kcal mol^{-1}, is close to the strength of one hydrogen bond. This seems reasonable as a hydrogen bond between the carbonyl group of 7-ketocholesterol and water needs to be broken when 7-ketocholesterol is pulled from the water phase into HDL. Both solutes get readily absorbed into the layer, and the 3 kcal mol^{-1} difference manifests in the PMF profiles in slightly different slopes at 3.4 nm < r < 5 nm but not in different overall shapes. We conclude that from the thermodynamic viewpoint, HDL should take up 7-ketocholesterol almost as easily as it does cholesterol. If there is any difference between cholesterol and 7-ketocholesterol in uptake from macrophages, there must be a specific selective mechanism at work, not considered in this study. Both cholesterol and 7-ketocholesterol are accessible to the solvent at their minimum energy positions and are, therefore, able to participate directly in signaling.

The convergence of simulation results for the minimum energies at r = 3.4 nm is demonstrated in Figure 5. We note that while the energies from independent simulations of the same molecule are not fully converged in the HDL core region, they converge at the important headgroup region, which is where the solutes are expected to be found. With the help of replica exchange (panel a), there is a clear trend for the energy to approach a converged value in all simulations. In the case of oxidized cholesterol, a timeframe of 60 ns per umbrella window is just enough to converge the energies being ultimately within 0.3 kcal mol^{-1} of each other.

By contrast to REUS, standard umbrella sampling simulations show no systematic convergence towards the REUS result for up to 20 ns per window. Although the REUS results do not fully converge in the first 20 ns either, they tend to move towards the converged value already during that time. Note that a detailed comparison of REUS and US has been done elsewhere.[44]

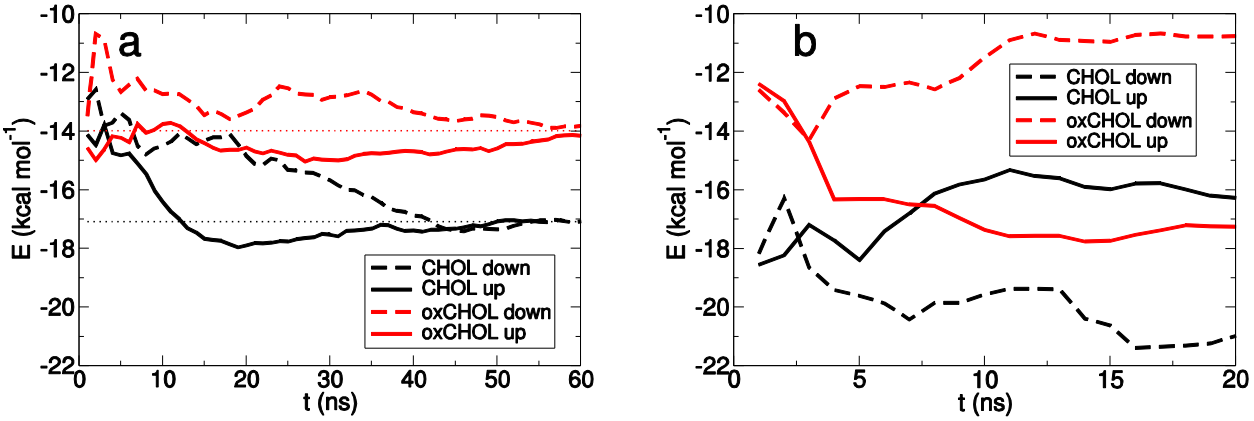

Figure 5. *Convergence of the free energy with simulation time, (panel a) with and (panel b) without replica exchange for cholesterol (CHOL) and 7-ketocholesterol (oxCHOL). The initial orientation is denoted in the same way as in Figure 4. The two dotted lines in panel a show the converged values, as defined by the final result from 60 ns REUS simulations, for cholesterol (black line) and 7-ketocholesterol (upper line).*

The orientational distributions of cholesterol and 7-ketocholesterol during the REUS simulations is shown in Figure 6. Comparing different initial headgroup orientations for the same molecule (i.e., comparing panels a-b and c-d) we see that neither cholesterol nor 7-ketocholesterol is able to reorient in the core of HDL during the simulations. There is less packing in the POPC headgroup region, which allows cholesterol and 7-ketocholesterol to immediately reorient there such that their tails point towards the HDL core and their headgroups make contact with POPC headgroups. This is demonstrated by the absence of signal in Figure 6 of angles over 100° in this region, even in simulations where the headgroup is initially pointing down.

A small but very densely sampled spot is seen at 2.8 nm and 100° in the cholesterol headgroup down simulation (panel a). This spot corresponds to a locally favorable position and orientation to

which the cholesterol molecule is strongly attracted, as evidenced by the PMF profile and the fact that the 100° angle is so heavily sampled at r = 2.8 nm.

Neither cholesterol nor 7-ketocholesterol reorients from a headgroup up to a headgroup down orientation in the particle core during the 60 ns of REUS. No preferred orientation is expected to be found in this region of HDL, where the hydrophobic core lipids form a disordered melt. Therefore, one would expect a uniform orientational sampling in this area in the limit of very long simulation times. The observed lack of convergence of orientational sampling in this region is not surprising given the extremely long correlation times of lipid movements in this region.

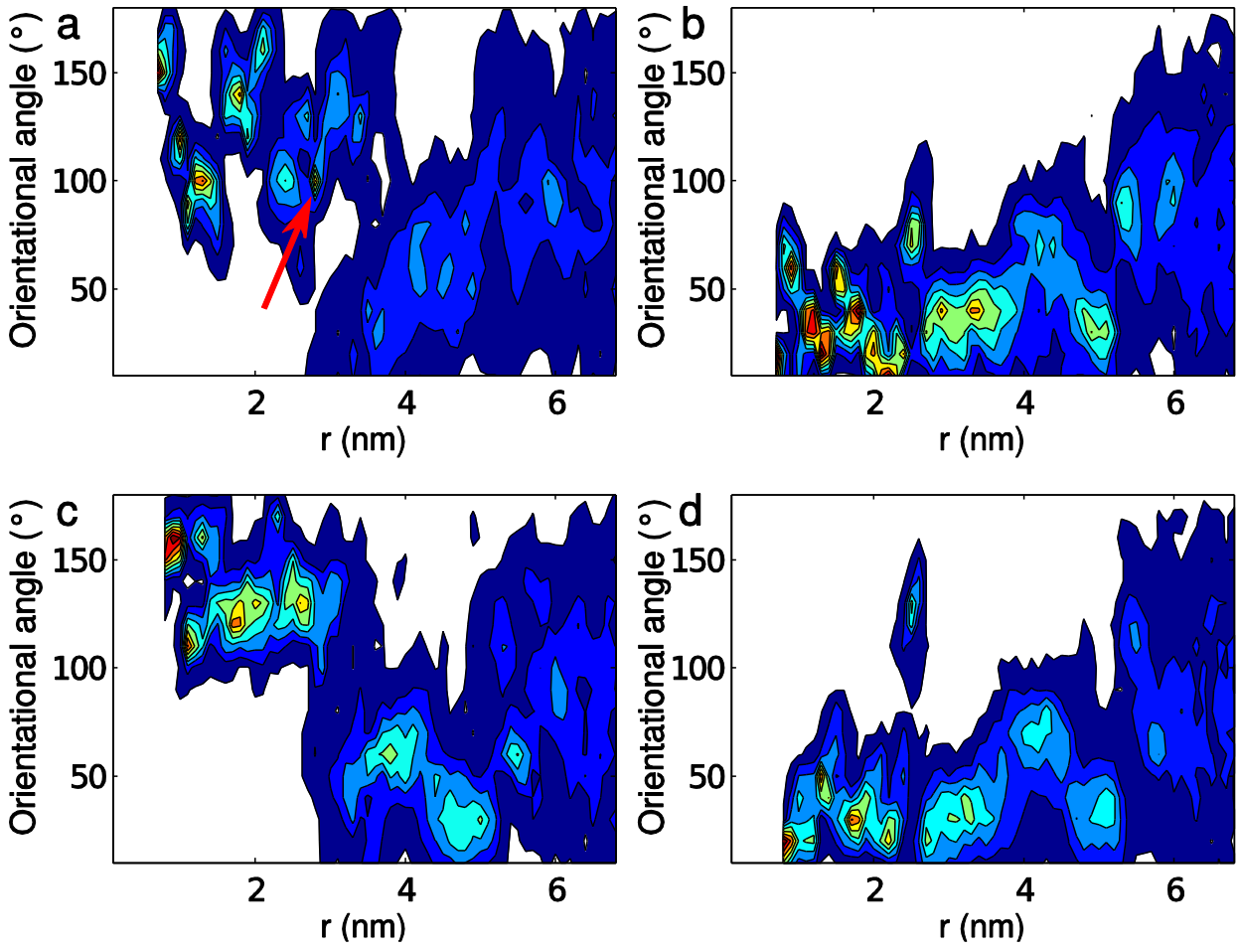

Figure 6. *Orientational sampling during REUS for cholesterol down (a), cholesterol up (b), 7-ketocholesterol down (c) and 7-ketocholesterol up (d), where "up" and "down" denote the initial*

headgroup orientation (see methods). The sampling scale is from dark blue (least sampling) to light blue, cyan, yellow, orange, red, and dark red. White areas are not sampled. At distances below 2.5 nm, the initial orientation essentially determines sampling throughout the simulation. Between 2.5 nm and 5 nm, the molecule tends to reorient so that the headgroup points upwards. At distances of 5 nm and higher, all orientations are sampled and a tangential orientation is slightly preferred. The red arrow in panel a marks the very densely sampled spot at 2.8 nm, 100°.

To detect hidden barriers caused by degrees of freedom orthogonal to the reaction coordinate *r*, we calculated the transmission factor ratio T_r^{ratio} at each umbrella window. The result is shown in Figure 7. The transmission factor is low in overall, which indicates that the replicas diffuse slowly between umbrella windows, and it actually goes to zero at many points for $r < 3$. A zero value means that no replicas travel through a 0.9 nm wide region centered at that umbrella position. Local exchange of replicas is still possible in these regions, but random walking of replicas through all umbrellas is not.

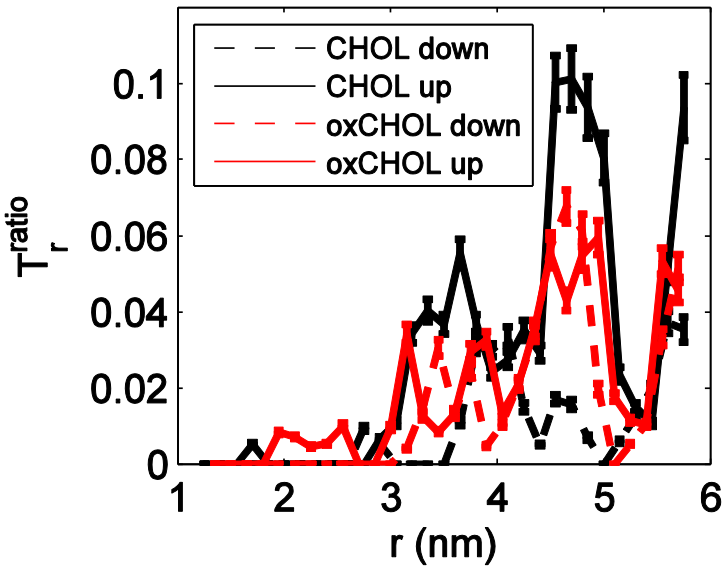

Figure 7. *The transmission factor ratio from 60 ns REUS simulations with different initial orientations of the solute. Standard deviations from the mean are shown with error bars. The low*

values below r = 3 nm indicate hidden sampling barriers orthogonal to the reaction coordinate r in that region. The simulation of cholesterol with the "headgroup down" initial orientation suffers from poor replica random walking at r < 3.5 nm.

The transmission factor ratio and the orientation distribution show that the simulation of cholesterol with the "headgroup down" initial orientation encounters significant sampling barriers at $r < 3.5$ nm, which supports our assumption that the lack of convergence of the cholesterol PMF curves at these distances (Figure 4) is an artifact due to insufficient sampling in the "headgroup down" simulation.

Conclusions

In this study, we constructed free energy profiles connected with the uptake of cholesterol and 7-ketocholesterol from an aqueous solution into an HDL particle. The employed replica exchange method helped to explore more efficiently the conformational space during umbrella sampling simulations, nevertheless, lengthy simulations were needed to obtain converged free energy profiles in the lipid environment. We demonstrated in quantitative terms the difference between cholesterol and 7-ketocholesterol adsorption to high-density lipoprotein with free energy minima of about -17 and -14 kcal/mol, respectively. We showed that both solutes are readily adsorbed by the HDL particle and end up in the same region at its surface.

On the basis of its position at the surface, HDL-bound 7-ketocholesterol is expected to be able to participate directly in biological signaling. Given that the structures of various oxysterols are quite similar, this suggests that other oxysterols also reside largely at the surface region of HDL and are potential candidates for signaling processes, too. Keeping in mind that the radial distribution of cholesterol in HDL and LDL particles is largely identical,[13,17] favoring the positioning of cholesterol close to the surface layer region of the lipoproteins, it is a plausible

suggestion that this view also holds for LDL. Finally, our study shows that free energy calculations together with the replica exchange method provide a useful and efficient approach for elucidating affinities of different sterols for lipoproteins. This result is interesting also given its importance for the study of fusion of lipoproteins and other lipid aggregates and the role of lipid oxidation in this complex process as part of initiation of atherosclerosis.

ACKNOWLEDGMENT

We are grateful to the Academy of Finland for financial support via the Finland Distinguished Professor (FiDiPro) program and the Center of Excellence program. PJ thanks also the Czech Science foundation (grant P208/12/G016) and the Academy of Sciences (Praemium Academiae award) for support. IV thanks the European Research Council (Advanced Grant project CROWDED-PRO-LIPIDS). TK thanks the Väisälä Foundation (grant for Ph.D. studies) for support. We wish to thank CSC – IT Center for Science (Espoo, Finland) for computing resources that rendered this work possible.

References

1. Lund-Katz, S.; Phillips, M. C. High Density Lipoprotein Structure-Function and Role in Reverse Cholesterol Transport. *Subcell. Biochem.* **2010,** *51,* 183–227.

2. Davidson, M. H.; Toth, P. P. High-Density Lipoprotein Metabolism: Potential Therapeutic Targets. *Am. J. Cardiol.* **2007,** *100,* 32N–40N.

3. Blanche, P. J.; Gong, E. L.; Forte, T. M.; Nichols, A. V. Characterization of Human High-Density Lipoproteins By Gradient Gel Electrophoresis. *Biochim. Biophys. Acta* **1981,** *665*, 408–419.

4. Huang, R.; Silva, R. A.; Jerome, W. G.; Kontush, A.; Chapman, M. J.; Curtiss, L. K.; Hodges, T. J.; Davidson, W. S. Apolipoprotein A-I Structural Organization in High-Density Lipoproteins Isolated From Human Plasma. *Nat. Struct. Mol. Biol.* **2011,** *18,* 416–422.

5. Rifici, V. A.; Khachadurian, A. K. Oxidation of High Density Lipoproteins: Characterization and Effects on Cholesterol Efflux From J774 Macrophages. *Biochim. Biophys. Acta* **1996,** *1299,* 87–94.

6. Bowry, V. W.; Stanley, K. K.; Stocker, R. High Density Lipoprotein Is the Major Carrier of Lipid Hydroperoxides in Human Blood Plasma From Fasting Donors. *Proc. Natl. Acad. Sci. U.S.A.* **1992,** *89,* 10316–10320.

7. Garner, B.; Witting, P. K.; Waldeck, A. R.; Christison, J. K.; Raftery, M.; Stocker, R. Oxidation of High Density Lipoproteins. *J. Biol. Chem.* **1998,** *273,* 6080–6087.

8. Kathir, K.; Dennis, J. M.; Croft, K. D.; Mori, T. A.; Lau, A. K.; Adams, M. R.; Stocker, R. Equivalent Lipid Oxidation Profiles in Advanced Atherosclerotic Lesions of Carotid Endarterectomy Plaques Obtained from Symptomatic Type 2 Diabetic and Nondiabetic Subjects. *Free Radic. Biol. Med.* **2010,** *49,* 481–486.

9. Aldrovandi, M.; O'Donnell, V. B. Oxidized PLs and Vascular Inflammation. *Curr. Atheroscler. Rep.* **2013,** *15,* 323.

10. Stemmer, U.; Hermetter, A. Protein Modification by Aldehydophospholipids and Its Functional Consequences. *Biochim. Biophys. Acta* **2012,** *1818,* 2436–2445.

11. Schroepfer, G. J. J. Oxysterols: Modulators of Cholesterol Metabolism and Other Processes. *Physiol. Rev.* **2000,** *80*, 361–554.

12. Iborra, R. T.; Machado-Lima, A.; Castilho, G.; Nunes, V. S.; Abdalla, D. S.; Nakandakare, E. R.; Passarelli, M. Advanced Glycation in Macrophages Induces Intracellular Accumulation of 7-ketocholesterol and Total Sterols by Decreasing the Expression of ABCA-1 and ABCG-1. *Lipids Health Dis.* **2011,** *10*, 172.

13. Vuorela, T.; Catte, A.; Niemelä, P. S.; Hall, A.; Hyvönen, M. T.; Marrink, S.-J.; Karttunen, M.; Vattulainen, I. Role of Lipids in Spheroidal High Density Lipoproteins. *PLoS Comput. Biol.* **2010,** *6*, e1000964.

14. Koivuniemi, A.; Vuorela, T.; Kovanen, P. T.; Vattulainen, I.; Hyvönen, M. T. Lipid Exchange Mechanism of the Cholesteryl Ester Transfer Protein Clarified by Atomistic and Coarse-grained Simulations. *PLoS Comput. Biol.* **2012,** *8*, e1002299.

15. Koivuniemi, A.; Vattulainen, I. Revealing Structural and Dynamical Properties of High Density Lipoproteins through Molecular Simulations. *Soft Matter* **2012,** *8*, 1262–1267.

16. Yetukuri, L.; Huopaniemi, I.; Koivuniemi, A.; Maranghi, M.; Hiukka, A.; Nygren, H.; Kaski, S.; Taskinen, M.-R.; Vattulainen, I.; Jauhiainen, M.; Orešič, M. High Density Lipoprotein Structural Changes and Drug Response in Lipidomic Profiles following the Long-Term Fenofibrate Therapy in the FIELD Substudy. *PLoS One* **2011,** *6*, e23589.

17. Murtola, T.; Vuorela, T. A.; Hyvonen, M. T.; Marrink, S.-J.; Karttunen, M.; Vattulainen, I. Low Density Lipoprotein: Structure Dynamics and Interactions of apoB-100 with Lipids. *Soft Matter* **2011,** *7*, 8135–8141.

18. Äijänen, T.; Koivuniemi, A.; Javanainen, M.; Rissanen, S.; Rog, T.; Vattulainen, I. How Anacetrapib Inhibits the Activity of the Cholesteryl Ester Transfer Protein? Perspective through Atomistic Simulations. *PLoS Comput. Biol.* **2014,** *10*, e1003987.

19. Sugita, Y.; Kitao, A.; Okamoto, Y. Multidimensional Replica-Exchange Method for Free-Energy Calculations. *J. Chem. Phys.* **2000,** *113*, 6042–6051.

20. Jorgensen, W. L.; Maxwell, D. S.; Tirado-Rives, J. Development and Testing of the OPLS All-Atom Force Field on Conformational Energetics and Properties of Organic Liquids. *J. Am. Chem. Soc.* **1996,** *118*, 11225–11236.

21. Jorgensen, W. L.; Chandrasekhar, J.; Madura, J. D.; Impey, R. W.; Klein, M. L. Comparison of Simple Potential Functions for Simulating Liquid Water. *J. Chem. Phys.* **1983,** *79*, 926–935.

22. Nosé, S. A Unified Formulation of the Constant Temperature Molecular Dynamics Methods. *J. Chem. Phys.* **1984,** *81*, 511–519.

23. Hoover, W. G. Canonical Dynamics: Equilibrium Phase-Space Distributions. *Phys. Rev. A* **1985,** *31,* 1695–1697.

24. Parrinello, M.; Rahman, A. Polymorphic Transitions in Single Crystals: a New Molecular Dynamics Method. *J. Appl. Phys.* **1981,** *52,* 7182–7190.

25. Hess, B.; Bekker, H.; Berendsen, H. J. C.; Fraaije, J. G. E. M. LINCS: a Linear Constraint Solver for Molecular Simulations. *J. Comput. Chem.* **1997,** *18*, 1463–1472.

26. Essmann, U.; Perera, L.; Berkowitz, M. L.; Darden, T.; Lee, H.; Pedersen, L. G. A Smooth Particle Mesh Ewald Method. *J. Chem. Phys.* **1995,** *103,* 8577–8592.

27. Roux, B. The Calculation of the Potential of Mean Force Using Computer Simulations. *Comput. Phys. Commun.* **1995,** *91,* 275–282.

28. Torrie, G.; Valleau, J. Nonphysical Sampling Distributions in Monte Carlo Free-Energy Estimation: Umbrella Sampling. *J. Comput. Phys.* **1977,** *23,* 187–199.

29. Kumar, S.; Bouzida, D.; Swendsen, R. H.; Kollman, P. A.; Rosenberg, J. M. The Weighted Histogram Analysis Method for Free-Energy Calculations on Biomolecules. I. The Method. *J. Comput. Chem.* **1992,** *13,* 1011–1021.

30. Neale, C.; Bennett, W. F. D.; Tieleman, D. P.; Pomès, R. Statistical Convergence of Equilibrium Properties in Simulations of Molecular Solutes Embedded in Lipid Bilayers. *J. Chem. Theory Comput.* **2011,** *7*, 4175–4188.

31. Neale, C.; Hsu, J. C. Y.; Yip, C. M.; Pomès, R. Indolicidin Binding Induces Thinning of a Lipid Bilayer. *Biophys. J.* **2014,** *106*, L29–L31.

32. Park, S.; Kim, T.; Im, W. Transmembrane Helix Assembly by Window Exchange Umbrella Sampling. *Phys. Rev. Lett.* **2012,** *108*, 108102.

33. Moradi, M.; Tajkhorshid, E. Mechanistic Picture for Conformational Transition of a Membrane Transporter at Atomic Resolution. *Proc. Natl. Acad. Sci. U.S.A.* **2013,** *110*, 18916–18921.

34. Lou, H.; Cukier, R. I. Molecular Dynamics of Apo-Adenylate Kinase: A Distance Replica Exchange Method for the Free Energy of Conformational Fluctuations. *J. Phys. Chem. B* **2006,** *110*, 24121–24137.

35. Wolf, M. G.; Jongejan, J. A.; Laman, J. D.; de Leeuw, S. W. Rapid Free Energy Calculation of Peptide Self-Assembly by REMD Umbrella Sampling. *J. Phys. Chem. B* **2008,** *112*, 13493–13498.

36. Murata, K.; Sugita, Y.; Okamoto, Y. Free Energy Calculations for DNA Base Stacking by Replica-Exchange Umbrella Sampling. *Chem. Phys. Lett.* **2004,** *385*, 1–7.

37. Curuksu, J.; Sponer, J.; Zacharias, M. Elbow Flexibility of the kt38 RNA Kink-Turn Motif Investigated by Free-Energy Molecular Dynamics Simulations. *Biophys. J.* **2009,** *97*, 2004–2013.

38. Kokubo, H.; Tanaka, T.; Okamoto, Y. Prediction of Protein–Ligand Binding Structures by Replica-Exchange Umbrella Sampling Simulations: Application to Kinase Systems. *J. Chem. Theory Comput.* **2013,** *9*, 4660–4671.

39. Kokubo, H.; Tanaka, T.; Okamoto, Y. Two-Dimensional Replica-Exchange Method for Predicting Protein–Ligand Binding Structures. *J. Comp. Chem.* **2013,** *34*, 2601–2614.

40. Jiang, W.; Luo, Y.; Maragliano, L.; Roux, B. Calculation of Free Energy Landscape in Multi-Dimensions with Hamiltonian-Exchange Umbrella Sampling on Petascale Supercomputer. *J. Chem. Theory Comput.* **2012,** *8*, 4672–4680.

41. Jacobitz, A. W.; Wereszczynski, J.; Yi, S. W.; Amer, B. R.; Huang, G. L.; Nguyen, A. V.; Sawaya, M. R.; Jung, M. E.; McCammon, J. A.; Clubb, R. T. Structural and Computational Studies of the Staphylococcus aureus Sortase B-Substrate Complex Reveal a Substrate-stabilized Oxyanion Hole. *J. Biol. Chem.* **2014,** *289*, 8891–8902.

42. Ostmeyer, J.; Chakrapani, S.; Pan, A. C.; Perozo, E.; Roux, B. Recovery from Slow Inactivation in K+ Channels Is Controlled by Water Molecules. *Nature* **2013,** *501*, 121–124.

43. Park, S.; Im, W. Two Dimensional Window Exchange Umbrella Sampling for Transmembrane Helix Assembly. *J. Chem. Theory Comput.* **2013,** *9*, 13–17.

44. Neale, C.; Madill, C.; Rauscher, S.; Pomès, R. Accelerating Convergence in Molecular Dynamics Simulations of Solutes in Lipid Membranes by Conducting a Random Walk along the Bilayer Normal. *J. Chem. Theory Comput.* **2013,** *9*, 3686–3703.

45. Hess, B.; Kutzner, C.; van der Spoel, D.; Lindahl, E. GROMACS 4: Algorithms for Highly Efficient, Load-Balanced, and Scalable Molecular Simulation. *J. Chem. Theory Comput.* **2008,** *4* , 435–447.

46. Hub, J. S.; de Groot, B. L.; van der Spoel, D. g_wham —A Free Weighted Histogram Analysis Implementation Including Robust Error and Autocorrelation Estimates. *J. Chem. Theory Comput.* **2010,** *6*, 3713–3720.

Table of Contents Graphic